Video Article

# A Rhodopsin Transport Assay by High-Content Imaging Analysis

Bing Feng[1], Xujie Liu[1], Yuanyuan Chen[1,2]

[1]Department of Ophthalmology, University of Pittsburgh

[2]McGowan Institute for Regenerative Medicine, University of Pittsburgh

Correspondence to: Yuanyuan Chen at Yuanyuan.Chen@pitt.edu

URL: https://www.jove.com/video/58703
DOI: doi:10.3791/58703

Keywords: High-content imaging, misfolded protein, rhodopsin, retinitis pigmentosa, pharmacological chaperone, immunostaining

Date Published: 12/13/2018

Citation: Feng, B., Liu, X., Chen, Y. A Rhodopsin Transport Assay by High-Content Imaging Analysis. *J. Vis. Exp.* (), e58703, doi:10.3791/58703 (2018).

## Abstract

Rhodopsin misfolding mutations lead to rod photoreceptor death that is manifested as autosomal dominant retinitis pigmentosa (RP), a progressive blinding disease that lacks effective treatment. We hypothesize that the cytotoxicity of the misfolded rhodopsin mutant can be alleviated by pharmacologically stabilizing the mutant rhodopsin protein. The P23H mutation, among the other Class II rhodopsin mutations, encodes a structurally unstable rhodopsin mutant protein that is accumulated in the endoplasmic reticulum (ER), whereas the wild type rhodopsin is transported to the plasma membrane in mammalian cells. We previously performed a luminescence-based high-throughput screen (HTS) and identified a group of pharmacological chaperones that rescued the transport of the P23H rhodopsin from ER to the plasma membrane. Here, using an immunostaining method followed by a high-content imaging analysis, we quantified the mutant rhodopsin protein amount in the whole cell and on the plasma membrane. This method is informative and effective to identify true hits from false positives following HTS. Additionally, the high-content image analysis enabled us to quantify multiple parameters from a single experiment to evaluate the pharmacological properties of each compound. Using this assay, we analyzed the effect of 11 different compounds towards six RP associated rhodopsin mutants, obtaining a 2-D pharmacological profile for a quantitative and qualitative understanding about the structural stability of these rhodopsin mutants and efficacy of different compounds towards these mutants.

## Video Link

The video component of this article can be found at https://www.jove.com/video/58703/

## Introduction

Protein misfolding is involved in muscular dystrophy, neural degenerations, as well as blinding diseases, including retinitis pigmentosa (RP)[1]. RP is an inherited and progressive retinal degeneration associated with mutations in over 60 genes affecting the function and homeostasis of rod photoreceptors or the retinal pigmented epitheliums (RPEs)[2,3]. No effective treatment is currently available for RP. *Rhodopsin* mutations account for about 25-30% of autosomal dominant (ad) RP cases. Among the more than 150 *Rhodopsin* mutations[4] (Human Gene Mutation Database, http:/www.hgmd.cf.ac.uk/), the Class II mutations cause the structural instability of the rhodopsin protein that contributes to the rod photoreceptor death and vision loss[5,6,7,8]. The P23H is the most frequent *Rhodopsin* mutation in North America, which is also a typical example of the Class II rhodopsin mutations[9,10]. Due to its inherent structural instability, the misfolded rhodopsin is accumulated in the endoplasmic reticulum (ER) in mammalian cells, whereas the wild type rhodopsin is located on the plasma membrane[5]. The misfolded rhodopsin P23H mutant exhibits dominant negative cytotoxicity that is not due to haploinsufficiency, but is related to the activation of ER associated protein degradation pathway and the interrupted rod outer segment organization. To alleviate rod photoreceptor cell stress, one strategy is to stabilize the native folding of the mutant rhodopsin using a pharmacological chaperone.

To achieve this goal, we performed a cell-based high-throughput screen (HTSs)[11,12,13] using a β-galactosidase fragment complementation assay to quantify the P23H rhodopsin mutant transported on the plasma membrane. The robust and simple protocol of this HTS assay enabled us to explore the activities of about 79,000 small molecules for each screen. However, because this HTS assay reads luminescence signals, false positives including the β-gal inhibitors, colored or cytotoxic compounds are included in the hit list waiting to be identified by a secondary assay.

The traditional immunostaining and fluorescence imaging methods have been used for years to study the rhodopsin transport in mammalian cells[5,14,15,16]. However, these conventional methods cannot be used to quantify pharmacological effects of more than 10 compounds towards rhodopsin transport because a reliable imaging analysis requires a large number of images taken under a highly consistent condition, which is not amendable by the conventional imaging methods. Here, we developed an immunostaining based high-content imaging protocol as a secondary assay to quantify the cell surface transport of misfolded rhodopsin mutants[11,13,17]. To label rhodopsin on the plasma membrane, we skipped the step of cell membrane permeabilization and immunostained the rhodopsin mutants by a monoclonal (B6-30) anti-rhodopsin recognizing the N-terminal epitope of rhodopsin at the extracellular side of the cell membrane[18]. To visualize the mutant rhodopsin in the whole cell, we fused rhodopsin with the Venus fluorescence protein. By the quantification of the fluorescence intensities in different fluorescence channels, we are able to obtain multiple parameters from one single experiment including the total rhodopsin intensity in the whole cell, on the cell surface, and the ratio of rhodopsin fluorescence on the cell surface to that in the whole cell. Applying this method to stable cells expressing a total of six misfolded rhodopsin mutants, we can generate a pharmacological profile of multiple small molecule chaperones towards these

Copyright © 2018 Journal of Visualized Experiments 

mutants. In this protocol, all cells are immunostained in a 384-well plate and imaged using an automated imaging system under a highly consistent imaging condition. An image analysis is performed to each well, containing images of more than 600 cells to reduce variation due to the heterogeneity of the cells with varying cell shape and protein expression level. The workflow of this protocol is summarized in **Figure 1**. The advantage of this method is that we obtain high-resolution images as well as multi-parameter quantifications from the image-based analysis. In general, this protocol can be modified and applied to quantify the transport of any misfolded membrane protein of interest.

## Protocol

NOTE: The rhodopsin transport assay.

# 1. Preparation and Culture of Cells

1. Revive cryo-preserved U2OS stable cells expressing the wild type (WT) or mutant mouse rhodopsin-Venus fusion proteins. Thaw the cells at 37 °C until only small ice crystals are left in the vial.
   NOTE: The U2OS cells are used in this protocol because there is no photoreceptor cell line available for *in vitro* studies and the pre-ciliary biosynthesis of rhodopsin is regulated by similar molecular mechanisms in mammalian cells. Additionally, the U2OS cells attach tightly to the bottom of the plate and have large cell bodies, so they are ideal for the rhodopsin transport assay. Seven U2OS stable cells expressing the WT, T4R, P23H, P53R, C110Y, D190N and P267L rhodopsin mutants are used here as an example to show the quality and reliability of the assay. Stable cells expressing other rhodopsin mutants or other membrane proteins can be used, depending on the goal of the assay. Stable cells expressing human rhodopsin can be used in this assay if available. The mouse rhodopsin was used here because mouse and human rhodopsin proteins share 95% homology, and the compounds identified by this assay will be tested *in vivo* using a mouse adRP model carrying the rhodopsin P23H mutation[8]. The stable cells were generated as described previously[19]. The WT and mutant rhodopsin transcripts were quantified by q-PCR, and the clones of stable cells expressing similar levels of WT and mutant rhodopsin transcripts were selected for this assay. The expression of rhodopsin proteins was confirmed by immunoblot and immunostaining. The passage of cells used in this assay should be lower than 20.
2. Transfer each line of cells into a 15 mL conical tube containing 10 mL of growth medium (high glucose Dulbecco's modified Eagle's medium (DMEM) with 10% fetal bovine serum (FBS) and 5 µg/mL Plasmocin).
3. Centrifuge the tube at 200 x g for 5 min. Discard the supernatant and resuspend the cell pellet with 5 mL of cell growth medium for each cell line. Transfer each line of cell suspension into a 60 mm tissue culture dish and incubate at 37 °C with 5% $CO_2$.
4. Subculture the cells when the tissue culture dish reaches 90% confluence as described in reference[12].

# 2. Seeding Cells at 5,000 cells per Well

NOTE: Perform the following procedures in a tissue culture hood.

1. Treat the plate with poly-lysine.
   1. One day before seeding the cells, treat a black-wall and clear bottom 384-well plate with 20 µL/well of poly-lysine solution for 30 min.
   2. Aspirate the liquid and allow all wells to dry for 1 h. Put back the plate lid and store the plate at 4 °C overnight for cell seeding.

2. Prepare the cell suspension.
   1. Culture each cell line in growth medium in a 100 mm tissue culture dish until 90% confluence.
   2. Wash each dish with phosphate buffered saline (PBS) and detach the cells with 1 mL of 0.05% Trypsin at room temperature.
   3. Resuspend each line of cells in 10 mL of assay medium (high-glucose DMEM with 10% FBS,100 units/mL penicillin and 100 µg/mL streptomycin).
   4. Count the cells and dilute each line of cells to 1.25 ´ $10^4$ cells/mL with the assay medium.

3. Seed the cells.
   1. Use an electronic multichannel pipette or an automated reagent dispenser to dispense 40 µL/well of the cell suspension to three columns per cell line and fill columns 1-21 of the 384-well plate (**Figure 2**).
   2. Add 40 µL/well of U2OS (P23H-Rhodopsin-Venus) to columns 22-23 and 40 µL/well of U2OS (Rhodopsin-Venus) to column 24, as controls.
   3. Centrifuge the plate at 300 x g for 30 s to bring down all cells to the bottom of the 384-well plate.
      NOTE: Avoid physical shock to the plate after cell seeding. Otherwise, cells will be crushed to one corner of each well, and the plate will not be suitable for high-content imaging.
   4. Incubate the 384-well plate at 37 °C with 5% $CO_2$ for 3 h for the cells to attach to the bottom of the plate.

# 3. Treating the Cells with Compounds

1. Generate a plate map with treatment conditions as shown in **Figure 2**.
2. Prepare 300 µL of 5x working solutions of up to 15 compounds in a 96-well plate.
   1. Dilute cps 1 to 15 with the assay medium to five times of their final concentrations in wells A1 to G2 of the 96-well plate (**Figure 2A**). Add 300 µL of assay medium in well H2.
      NOTE: The final concentration of each compound is used at the most effective concentration for rescuing the transport of the P23H rhodopsin by the HTS[12,13].
   2. Add 100 µL per well of 2% dimethyl sulfoxide (DMSO) and 25 µM 9-*cis*-retinal that are diluted in the assay medium to columns 11 and 12, respectively. Add 9-*cis*-retinal in dim light.

Copyright © 2018 Journal of Visualized Experiments

3. Adding 10 µL per well of 5x working solutions to the 384-well plate cultured with the cells (**Figure 2B**).
    1. Use an electronic multi-channel pipette to add compounds 1, 3, 5, 7, 9, 11, 13, and 15 to rows A, C, E, G, I, K, M, and O from columns 1 to 21 (**Figure 2**). Add compounds 2, 4, 6, 8, 10, 12, 14 and M to rows B, D, F, H, J, L, N, and P from columns 1 to 21.
    2. Add 10 µL per well of 2% DMSO to columns 22 and 24. Add 10 µL per well of 25 µM 9-*cis*-retinal to column 23.
    NOTE: DMSO is used as a vehicle control because all the compounds are initially dissolved in DMSO as stocks. Column 22 containing DMSO treated cells expressing the P23H rhodopsin is used as the 0% control. 9-*Cis*-retinal treated cells expressing the P23H rhodopsin is used as the 100% control.

4. Cover the 384-well plate with aluminum foil and incubate the plate at 37 °C for 24 h.

## 4. Immunostaining without Membrane Permeabilization to Stain Rhodopsin Protein on the Cell Surface.

NOTE: Avoid any detergent in the entire immunostaining process to keep cell membrane intact.

1. Prepare 4% paraformaldehyde (PFA) by diluting the 16% PFA with PBS in a 1:4 volume ratio in a chemical fume hood. Transfer the 4% PFA in a reagent reservoir.
2. Take out the 384-well plate in a dark room with dim red light. Use an 8-channel aspirator connected to a vacuum collection bottle to gently aspirate the medium. Use an electronic multichannel pipette to add 20 µL per well of freshly prepared 4% PFA to the entire 384-well plate and incubate for 20 min at room temperature. To avoid cell detachment, always point the tips of the aspirator to the same side of each well during aspirations. Do not touch the middle bottom area of each well. When taking images, select fields to avoid the region touched by the aspirator. For incubations longer than 10 min, cover the 384-well plate with its lid to avoid evaporation.
NOTE: Cells are fixed in a dark room to avoid photobleaching of the regenerated isorhodopsin that will affect the result of the 100% control. After fixation, the 384-well plate can be taken out under normal light.
3. Use an 8-channel aspirator to aspirate the PFA in each well and use an electronic multi-channel pipette to add 50 µL per well of PBS. Repeat two more times to perform three washes with PBS.
CAUTION: The waste liquid containing PFA are collected in a capped bottle and is to be disposed of as a hazardous chemical waste after the experiment.
4. Block the cells by adding 20 µL per well of 5% goat serum to the entire 384-well plate and incubate at room temperature for 30 min.
5. Aspirate the 5% goat serum and add 15 µL per well of 20 µg $mL^{-1}$ B6-30 anti-rhodopsin antibody in 1% goat serum to rows A to O. Add 15 µL per well of 1% goat serum to row P for the secondary antibody-only control group.
6. Incubate the 384-well plate at room temperature for 90 min or at 4 °C overnight. Cover the 384-well plate with aluminum foil to avoid photobleaching of the fluorophores.
7. Wash the plate 3 times with 50 µL per well of PBS.
8. Aspirate PBS and add 15 µL per well of 5 µg $mL^{-1}$ Cy3-conjugated goat anti-mouse IgG antibody. Cover the 384-well plate with aluminum foil and incubate at room temperature for 1 h or at 4 °C overnight.
9. Wash the plate 3 times with 50 µL per well of PBS. Add 50 µL per well of PBS containing 1 µg $mL^{-1}$ Hoechst 33342 to stain nuclei at room temperature for 15 min.
10. Seal the 384-well plate with a transparent film before imaging. Cover the 384-well plate with aluminum foil and store at 4 °C for up to a week if images are taken immediately.

## 5. Imaging.

NOTE: This high-content imaging procedure is adapted to the imaging system listed in the **Table of Material**. Procedures can be different if using other high-content imaging systems.

1. Remove the lid and put the 384-well plate into the high-content imager with A1 positioned on the top left corner of the plate.
2. Open the image acquisition software to set up parameters for image acquisition.
    1. Open the Plate Acquisition Setup window and create new setting or load an existing setup file.
    2. Select the 20X objective and set up pixel binning as 2 so the calibrated pixel size is 0.80 ´ 0.80 µm. Set the scan lines as 2000 and the image size (W X H) as 1000 X 1000 pixels (800.00 ´ 800.00 µm) per site.
    3. Select the plate type to be imaged. Use the information provided by the manufacturer of the 384-well plate to fill in the plate dimensions.
    4. Select the wells to be imaged for the 384-well plate.
    5. Select four sites to be imaged per well. Avoid the side of the well touched by the aspiration tips.
    6. Select excitation lasers as 405, 488 and 561 nm. Select emission filters for DAPI, FITC and Texas Red channels. Optimize the laser power and gains of each channel to ensure the brightness of images taken from the positive control wells are less than the saturation threshold.
    7. Select well-to-well focus for autofocus. Select the first well acquired as the initial well for finding samples. Set site autofocus to all sites.
    8. Select four averages per line for each channel. Optimize the Z-offset value for each channel.
    9. Test 2-3 wells at the diagonal corners of the 384 well plate to make sure the images are on focus for all tested wells, images from all sites per well have cells with more than 40% confluence, and fluorescence intensities of all channels are about half saturated in the 100% control wells.
    10. Save the image acquisition method.

3. Run the entire plate. Watch the imager until it finishes capturing images from the first column of the plate to double-check the image quality before leaving the imager. Take the 384-well plate out and store at 4 °C for future use.

NOTE: Depending on the number of sites selected per well and the channels taken, it takes 40 min to 3 h to finish imaging one 384-well plate.

## 6. Image Analysis.

1. Pull out the image data using a high-content image analysis software. Select one of the 100% control wells (column 23) to set up parameters.
2. Select the **Multi-Wavelength Cell Scoring** as the analysis method and start configuring settings.
    1. Define the nuclei using images from the DAPI channel. Preview to make sure the defined nuclei shapes in the selected well fits well with the nuclei images.
    2. Define the shape of cell in the FITC channel where rhodopsin-Venus is imaged.
    3. Define the rhodopsin cell surface stain areas in the Texas Red channel.
    4. Test the current algorithm in 5 wells to determine if the settings are optimized. Save the settings and close the **Configuration** window.
3. Run all the wells with the optimized analysis method.
4. Export **Object Number** as intact cell number. Export the **Average Intensity** of the FITC channel as Rhodopsin-Venus Intensity (Rhodopsin-Venus INT). Export the **Average Intensity** of the Texas Red channel as rhodopsin intensity on the cell surface (Rhodopsin INT on the cell surface).
5. Open the exported data in a spreadsheet software. Divide the rhodopsin intensity on the cell surface by the rhodopsin-Venus INT as MEM-to-total ratio. Calculate the Z'-factors for each parameter to evaluate the assay quality. $Z'=1-3X(STD_{100\%\ control}+STD_{0\%\ control})/|Mean_{100\%\ control}-Mean_{0\%\ control}|$.
   NOTE: A Z'-factor higher than 0 indicates a moderate assay sufficient for a high-content screen, and a Z' factor between 0.5 and 1 suggests an outstanding assay required for a high-throughput screen[20,21].
6. Use the spreadsheet software to generate a two-color heat map for each parameter. Arrange the name of cell lines on the X-axis and the compounds on the Y-axis.

## Representative Results

We characterized the rhodopsin transport with three parameters: the rhodopsin-Venus intensity in the whole cell (Rhodopsin-Venus INT), the immunostaining intensity of rhodopsin on the plasma membrane (Rhodopsin INT on the cell surface), and the ratio of rhodopsin stain on the cell surface to rhodopsin-Venus intensity in the whole cell (MEM-Total Ratio). A representative result of the rhodopsin transport assay is shown in **Figure 3** and **Figure 4**. Using DMSO and 9-*cis*-retinal treated cells expressing the P23H-rhodopsin-Venus as the 0 and 100% controls, respectively, the Z'-factors for these three parameters are in the range between 0 to 0.5, suggesting that the assay has moderate quality, sufficient for high-content imaging[21]. Even though the optimized Z'-factors are lower than 0.5 due to its relatively complex procedures compared to a HTS assay, this assay is still robust and reliable for an image-based analysis. An active compound that rescues a misfolded rhodopsin should show higher values of Rhodopsin INT on the cell surface and MEM-Total Ratio than DMSO, with a *P* value lower than 0.05. Three 2-D heat maps were generated from these three parameters to compare the average rhodopsin amount and localization per cell (**Figure 4**). Repeated in triplicates, WT and six rhodopsin mutants are listed horizontally, and the effects of compound treatments are compared vertically. In agreement with previous studies, the rhodopsin INT on the cell surface and the MEM-Total ratio of are lower for the six mutants compared to the WT rhodopsin treated with DMSO (**Figure 4C**)[5,22,23]. The rhodopsin INT on the cell surface and its MEM-to-Total ratio are increased by 9-*cis*-retinal treatment for the T4R, P23H, D190N and P267L, but not the P53R or C110Y mutants, suggesting that 9-*cis*-retinal rescues the transport of the T4R, P23H, D190N and P267L rhodopsin mutants. All the cps showed varying levels of increase in the Rhodopsin INT on the cell surface for the T4R, P23H and D190N. Cps 3, 4, 5, 7, 8 and 11 increased the rhodopsin-Venus INT but not the MEM-to-Total ratio of these rhodopsin mutants, suggesting that these compounds only increased the rhodopsin amount. Cps 1, 2 6 and 9 significantly increased the MEM-to-Total ratio of T4R, P23H, D190N and P267L rhodopsin mutants, suggesting that these compounds rescue the transport of these rhodopsin mutants to the plasma membrane. The 2-D profiles provide a comprehensive overview of rhodopsin transport affected by these adRP associated mutations that are mitigated by different pharmacological treatment.

Copyright © 2018 Journal of Visualized Experiments

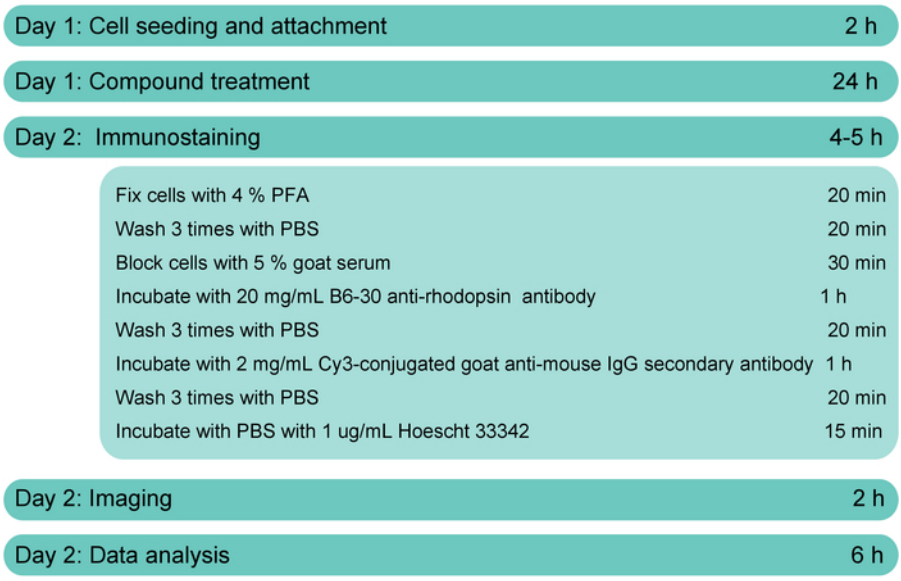


**Figure 1: The workflow of the rhodopsin transport assay.** Procedures for cell surface staining of rhodopsin without membrane permeabilization for the rhodopsin transport assay. Please click here to view a larger version of this figure.

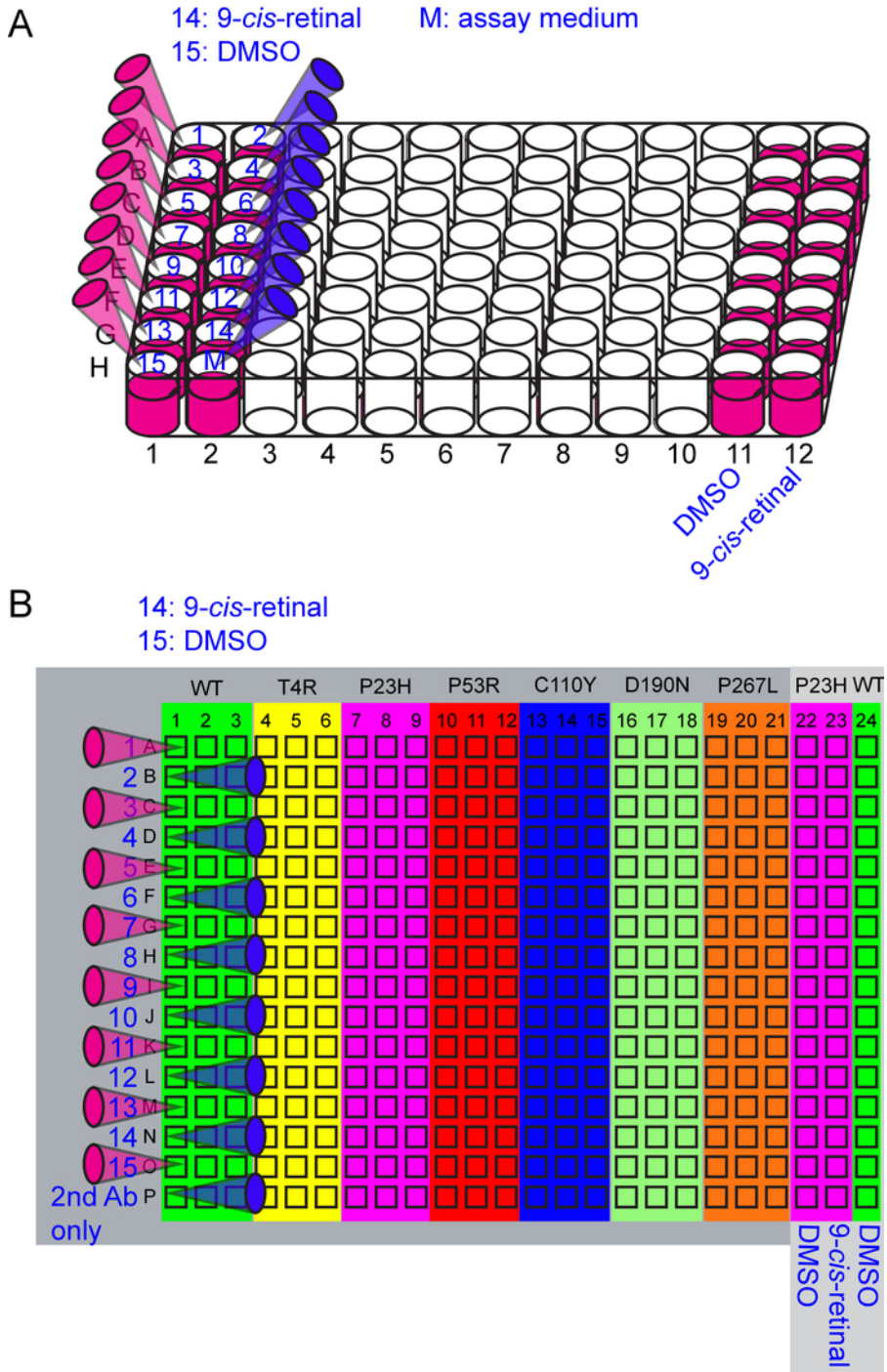


**Figure 2: Illustrations for the preparation of 5x working solutions and the liquid transfer from the 96-well plate to the 384-well plate.** (A) The 96-well plate layout of the 5x working solutions. Wells A1 to G2 have 300 µL per well of up to 15 5x working solutions and assay medium (M) as illustrated in columns 1 and 2. Compounds 14 and 15 are 2% DMSO and 25 µM 9-*cis*-retinal, respectively, for the treatment to the seven cell lines expressing WT and mutant rhodopsin. Additionally, columns 11 and 12 have 100 µL per well of 2% DMSO and 25 µM 9-*cis*-retinal controls, respectively, treated to the cells expressing the P23H rhodopsin for the calculation of Z'-factors. (B) The 384-well plate layout for cell type and treatment conditions. The U2OS cells expressing the WT, T4R, P23H, P53R, C110Y, D190N and P267L rhodopsin-Venus are seeded as illustrated. Treatment conditions are labeled in blue. Pink and blue tips demonstrate the well-to-well liquid transfer from the 96-well plate to the 384 plate using a multichannel pipette. Please click here to view a larger version of this figure.

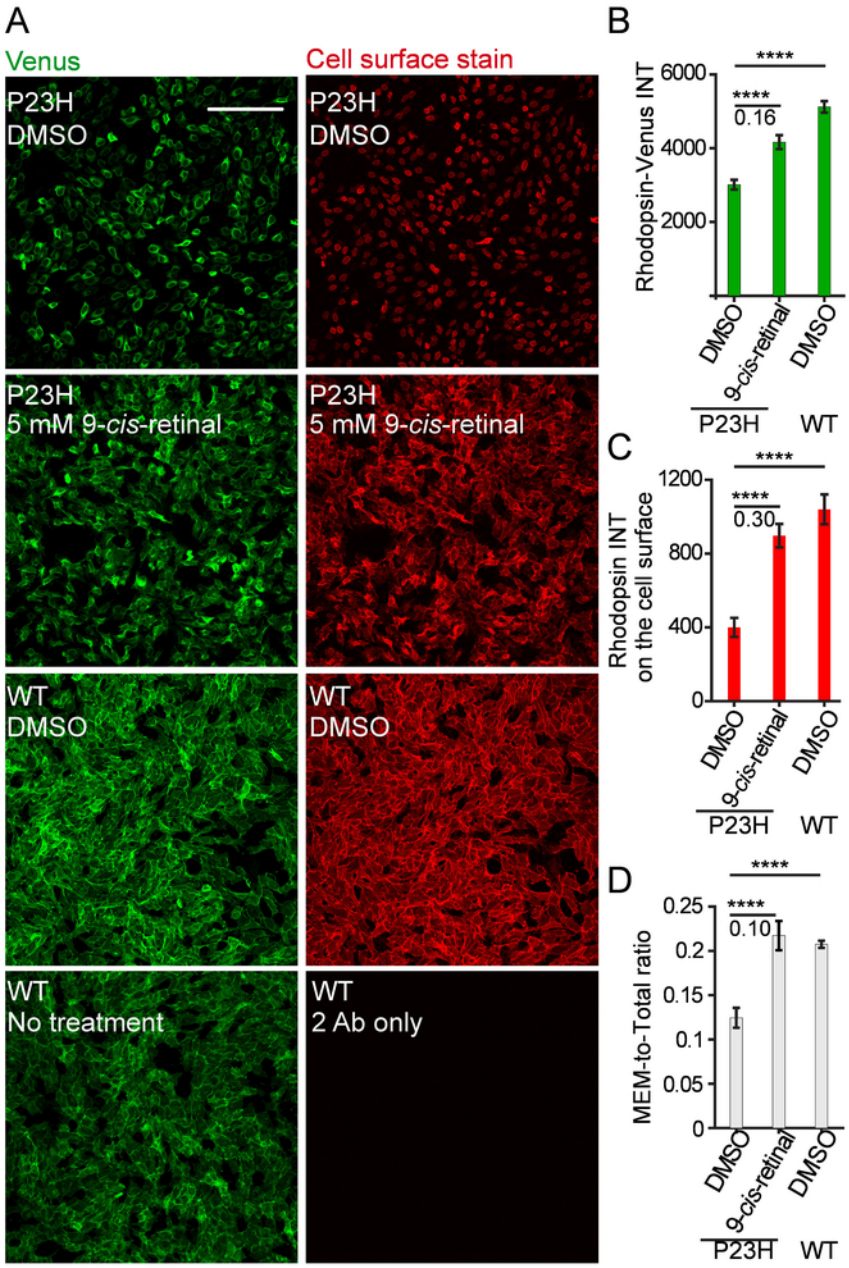


**Figure 3: Representative images and quantifications for the controls of the rhodopsin transport assay.** (A) Venus fluorescence (green) and cell surface immunostaining (red) of U2OS cells expressing WT or P23H rhodopsin-Venus treated with DMSO or 5 µM 9-*cis*-retinal. Scale bar = 200 µm. (B) A column plot of mean Venus intensity per cell representing rhodopsin amount in the whole cell (Rhodopsin-Venus INT). ****$p$<0.0001. Z'-factor is shown under the black line. Column value and error bar are average and standard deviation (S.D.) of 16 replicates, respectively. (C) A column plot of mean Cy3 intensity per cell representing the rhodopsin stained on the cell surface (Rhodopsin INT on the cell surface). (D) A column plot of the ratio of mean cy3 intensity per cell to mean Venus intensity per cell representing the ratio of rhodopsin level on the cell surface to its whole-cell level (MEM-to-total ratio). Please click here to view a larger version of this figure.

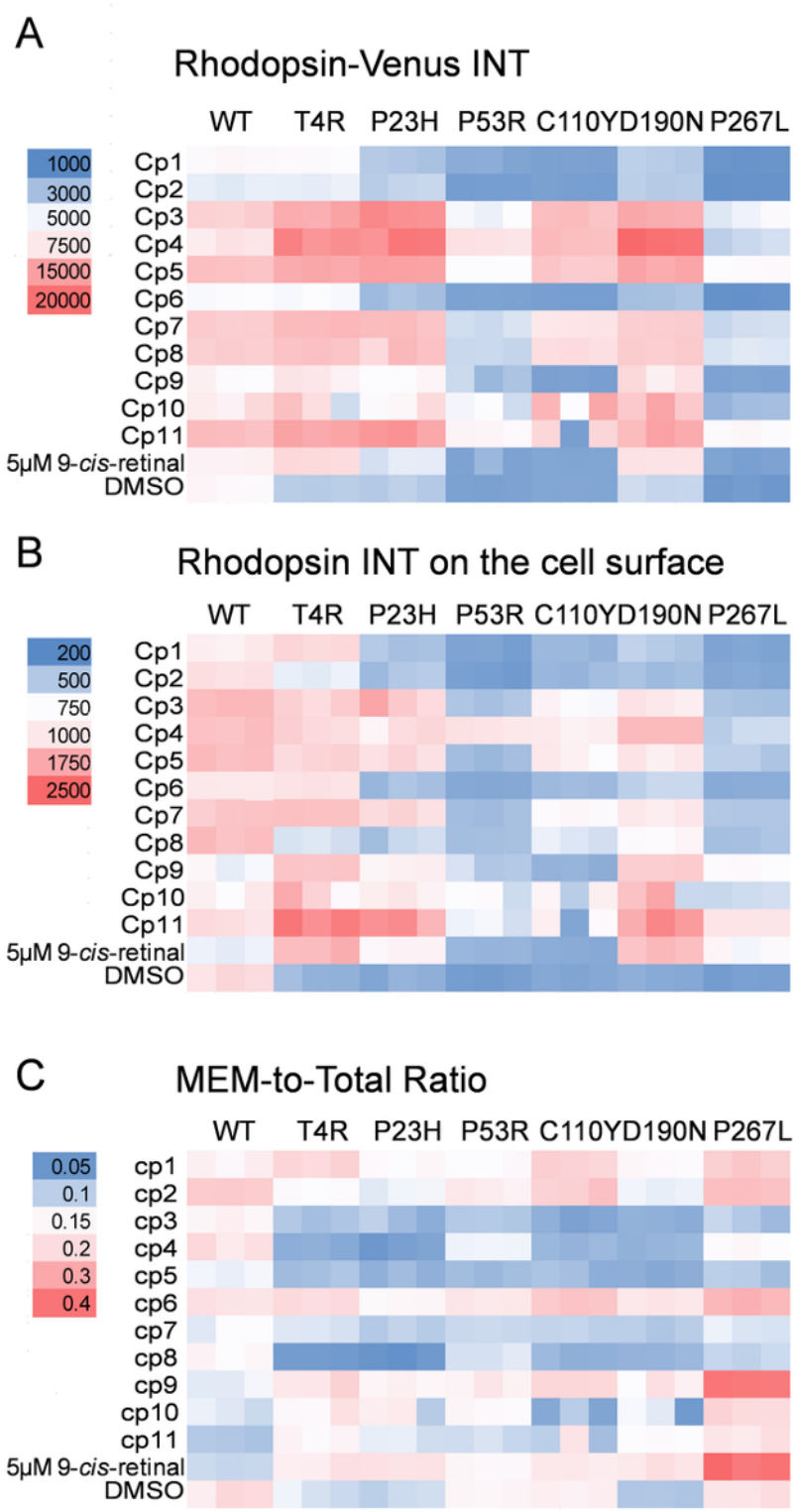


**Figure 4: A representative high-content analysis of the rhodopsin transport assay shown as 2-color heat maps.** (A) The heat map of mean Venus intensity per cell representing the whole-cell rhodopsin level (Rhodopsin-Venus INT). Each block represents a data point and each condition was tested in triplicate. The color legend is shown on the left. Cp, compound. (B) The heat map of mean Cy3 intensity per cell representing the rhodopsin stained on the cell surface (Rhodopsin INT on the cell surface). (C) The heat map of the mean Cy3 intensity per cell to the mean Venus intensity per cell representing the ratio of rhodopsin level on the cell surface to its whole-cell level (MEM-to-total ratio). Please click here to view a larger version of this figure.

## Discussion

Here, we showed a high-content imaging assay used for characterizing hits identified from a HTS. The only automation involved in these protocols is the high-content imager. The immunostaining and fluorescence imaging of rhodopsin have been used commonly to characterize the localization of rhodopsin[5,14,15,16]. However, the quantification of images taken by the traditional imaging methods is limited by the lack of sufficient cell images per condition, low capacity of images per experiment, and lack of a quality control parameter. We adapted the traditional immunostaining protocol to the 384-well format and replaced the traditional imaging with high-content imaging. Using this high-content imaging protocol, we successfully selected and characterized the activities of hits identified by a HTS[11,13,17]. Compared to the traditional immunostaining and imaging methods, this protocol significantly increased the consistence of imaging conditions, imaging capacity, and image analysis power, which enabled us to quantitatively compare the pharmacological effects of 11 compounds towards the transport of six adRP associated rhodopsin mutants.

The major changes of this protocol compared to the previously used protocols for rhodopsin immunostaining and imaging are: (1) growing and immunostaining cells in a clear-bottom 384-well plate; (2) imaging cells using a high-content imager; and (3) analyzing data with a high-content image analysis software. Due to these changes, an initial optimization is required to find the best cell seeding number, antibody concentrations, imaging conditions, and image analysis algorithms.

The critical steps of the protocol include: (1) seeding cells that allow 50-70% confluence before fixation; (2) careful aspirations to avoid cell detachment; (2) imaging several wells across the whole plate to make sure images are on focus and fluoresce of all channels does not exceed half of the threshold of the imager for the positive control wells before imaging the whole plate; and (3) keeping the Z'-factor higher than 0 to ensure the reliability of the assay.

The most common problems that could be encountered for this protocol are cell detachment and low Z'-factors. To avoid the first issue, pretreat the 384-well plate with poly-L-lysine to facilitate the cell attachment and avoid using cell lines that detach easily such as the Hek293 cells. Additionally, limit the aspiration tip to touch only one side of each well during aspiration and select the other side of each well for imaging. To improve the Z'-factor and the assay quality, optimize the cell seeding number and image analysis parameters to make sure the cell shape or nuclei shape defined by the software fits well with each object in each fluorescence channel.

Compared to other methods to quantify rhodopsin transport, such as a cell surface ELISA, or a β-galactosidase fragment complementation assay, which calculate the target protein level on the cell surface in all cells, this high-content imaging method quantifies average protein level per cell; and, this unique feature avoids a critical variation factor, cell number that affects the final readouts in other methods. Additionally, due to the large number of cells imaged and quantified by the high-content imaging method, the parameters averaged from all cells per well showed low variation between replicates, thus adding to the reliability of the assay.

One limitation of this protocol is that they are not the best assays for HTS, due to its relatively complicated procedure and the 2 h per plate imaging time. Thus, we recommend alternative reporter assays for screening large small-molecule libraries with more than 5,000 compounds, and use this high-content imaging protocol for focused characterization assays limited to less than 100 compounds. The second limitation of this protocol is its lack of standards to show whether the Venus fluorescence or the immunostaining fluorescence intensities are in a linear correlation with the quantity of rhodopsin protein amount per cell. To avoid saturation by immunostaining, we recommend testing and plotting the immunostaining intensities of the cells incubated with different concentrations of primary and secondary antibodies. Select the antibody concentrations within the linear range of florescence change.

Expanding from the current application, we will quantify rhodopsin transport from images of cells transiently transfected with 28 different rhodopsin mutants under treatment with up to 10 compounds to generate a pharmacological database of these compounds' activity for guidance of potential treatments to adRP patients carrying these rhodopsin mutations. This protocol can also be easily adapted to the translocation assays of any membrane protein of interest that will be useful for drug discoveries of other protein misfolding diseases.

## Disclosures

The authors have nothing to disclose.

## Acknowledgements

We thank Dr. Mark E. Schurdak and University of Pittsburgh Drug Discovery Institute for providing the high-content imager and initial trainings. Dr. Krzysztof Palczewski (Case Western Reserve University) generously shared the 1D4 and B630 anti-rhodopsin antibodies and the NIH3T3(Rhodopsin/GFP) and NIH3T3(P23H-rhodopsin/GFP) cells. The plasmid containing the cDNA of mouse rhodopsin-Venus construct was shared by Dr. Nevin Lambert (Augusta University). This work was supported by the National Institute of Health grant EY024992 to YC and P30EY008098 from University of Pittsburgh Vision Research Core grant.

## References

1. Gregersen, N., Bross, P., Vang, S., & Christensen, J. H. Protein misfolding and human disease. *Annual Review of Genomics and Human Genetics.* **7** 103-124, (2006).
2. Daiger, S. P., Bowne, S. J., & Sullivan, L. S. Perspective on genes and mutations causing retinitis pigmentosa. *Archives of Ophthalmology.* **125** (2), 151-158, (2007).
3. Daiger, S. P., Sullivan, L. S., & Bowne, S. J. Genes and mutations causing retinitis pigmentosa. *Clinical Genetics.* **84** (2), 132-141, (2013).

4. Stenson, P. D. *et al.* The Human Gene Mutation Database: towards a comprehensive repository of inherited mutation data for medical research, genetic diagnosis and next-generation sequencing studies. *Human Genetics.* **136** (6), 665-677, (2017).
5. Sung, C. H., Schneider, B. G., Agarwal, N., Papermaster, D. S., & Nathans, J. Functional heterogeneity of mutant rhodopsins responsible for autosomal dominant retinitis pigmentosa. *Proceedings of the National Academy of Sciences of the United States of America.* **88** (19), 8840-8844, (1991).
6. Athanasiou, D. *et al.* The molecular and cellular basis of rhodopsin retinitis pigmentosa reveals potential strategies for therapy. *Progress in Retinal and Eye Research.* **62** 1-23, (2018).
7. Chiang, W. C. *et al.* Robust Endoplasmic Reticulum-Associated Degradation of Rhodopsin Precedes Retinal Degeneration. *Molecular Neurobiology.* **52** (1), 679-695, (2015).
8. Sakami, S. *et al.* Probing mechanisms of photoreceptor degeneration in a new mouse model of the common form of autosomal dominant retinitis pigmentosa due to P23H opsin mutations. *Journal of Biological Chemistry.* **286** (12), 10551-10567, (2011).
9. Dryja, T. P. *et al.* Mutations within the rhodopsin gene in patients with autosomal dominant retinitis pigmentosa. *New England Journal of Medicine.* **323** (19), 1302-1307, (1990).
10. Sohocki, M. M. *et al.* Prevalence of mutations causing retinitis pigmentosa and other inherited retinopathies. *Human Mutation.* **17** (1), 42-51, (2001).
11. Chen, Y. *et al.* A novel small molecule chaperone of rod opsin and its potential therapy for retinal degeneration. *Nature Communications.* **9** (1), 1976, (2018).
12. Chen, Y., & Tang, H. High-throughput screening assays to identify small molecules preventing photoreceptor degeneration caused by the rhodopsin P23H mutation. *Methods in Molecular Biology.* **1271** 369-390, (2015).
13. Chen, Y. *et al.* A High-Throughput Drug Screening Strategy for Detecting Rhodopsin P23H Mutant Rescue and Degradation. *Investigative Ophthalmology & Visual Science.* **56** (4), 2553-2567, (2015).
14. Noorwez, S. M. *et al.* Pharmacological chaperone-mediated in vivo folding and stabilization of the P23H-opsin mutant associated with autosomal dominant retinitis pigmentosa. *Journal of Biological Chemistry.* **278** (16), 14442-14450, (2003).
15. Saliba, R. S., Munro, P. M., Luthert, P. J., & Cheetham, M. E. The cellular fate of mutant rhodopsin: quality control, degradation and aggresome formation. *Journal of Cell Science.* **115** (Pt 14), 2907-2918, (2002).
16. Kaushal, S., & Khorana, H. G. Structure and function in rhodopsin. 7. Point mutations associated with autosomal dominant retinitis pigmentosa. *Biochemistry.* **33** (20), 6121-6128, (1994).
17. Chen, Y., Brooks, M. J., Gieser, L., Swaroop, A., & Palczewski, K. Transcriptome profiling of NIH3T3 cell lines expressing opsin and the P23H opsin mutant identifies candidate drugs for the treatment of retinitis pigmentosa. *Pharmacological Research.* **115** 1-13, (2016).
18. Adamus, G. *et al.* Anti-rhodopsin monoclonal antibodies of defined specificity: characterization and application. *Vision Research.* **31** (1), 17-31, (1991).
19. Goodson, H. V., Dzurisin, J. S., & Wadsworth, P. Generation of stable cell lines expressing GFP-tubulin and photoactivatable-GFP-tubulin and characterization of clones. *Cold Spring Harbor Protocols.* **2010** (9), pdb prot5480, (2010).
20. Zhang, J. H., Chung, T. D., & Oldenburg, K. R. A Simple Statistical Parameter for Use in Evaluation and Validation of High Throughput Screening Assays. *Journal of Biomolecular Screening.* **4** (2), 67-73, (1999).
21. Bray, M. A., & Carpenter, A. Advanced Assay Development Guidelines for Image-Based High Content Screening and Analysis. In *Assay Guidance Manual* eds Sittampalam, G. S. *et al.* Bethesda (MD): Eli Lilly & Company and the National Center for Advancing Translational Sciences (2004).
22. Sung, C. H., Davenport, C. M., & Nathans, J. Rhodopsin mutations responsible for autosomal dominant retinitis pigmentosa. Clustering of functional classes along the polypeptide chain. *Journal of Biological Chemistry.* **268** (35), 26645-26649, (1993).
23. Krebs, M. P. *et al.* Molecular mechanisms of rhodopsin retinitis pigmentosa and the efficacy of pharmacological rescue. *Journal of Molecular Biology.* **395** (5), 1063-1078, (2010).


Copyright © 2018 Journal of Visualized Experiments 